Pergamon

Applied Geochemistry, Vol. 10, pp. 317–327, 1995
Elsevier Science Ltd
Printed in Great Britain
0883–2927/95 $9.50 + 0.00

0883–2927(95)00009–7

The influence of mineralogy and texture in the water content of rock salt formations. Its implication in radioactive waste disposal

C. De Las Cuevas and J. J. Pueyo

Laboratori d'Investigació en Formacions Salines, LIFS, Dept. de Geoquimica, Facultat de Geología, Universitat de Barcelona, 08028 Barcelona, Spain

(*Received* 22 *March* 1994; *accepted in revised form* 16 *February* 1995)

Abstract—The consideration of the use of salt formations as possible radioactive waste disposal sites led us to attempt to determine the extent to which their brine content could influence the performance of the disposal system. Bedded rock salt from the Cardona, Zaragoza and Guendulain Fms., as well as diapiric rock salt from northern and southeastern Spain, have been selected and their water contents characterized by thermogravimetry. Free water content (intergranular water and water in fluid inclusions) in the studied formations ranges from 0.01 to 1.24% weight. In addition, the presence of hydrated minerals increases the amount of total water in the rock (up to 3.50%). Clear differences between the studied formations are observed in the total amount of water and in the form of water entrapment in rock salt. The results obtained have allowed the classification of the studied rock salt formations with respect to their free-brine content as water-poor (around 0.1% in average), intermediate water-rich (around 0.2%) and water-rich (higher than 0.3%). The petrographical features of the rock salt, such as mineralogical content and halitic textures, play an important role in its water content. Whilst brine in fluid inclusions is related to the halite texture, intergranular brine depends mainly on the content of clay and sulphate minerals.

INTRODUCTION

The long-lived radionuclides present in radioactive wastes must be kept isolated from the Biosphere for time periods long enough so that their activity has decayed to levels at which their incorporation into the environment can be considered not to be hazardous. It is clear that such a constraint rules out any conception of waste containment based on man-made structures and human surveillance. The most accepted way to ensure containment of the wastes is by their disposal in deep geological formations.

The long-term safety of a high radioactive waste disposal site in a geological formation depends on the extent to which it is possible to avoid contact between groundwater and the waste itself. Understanding the mechanisms involved in the migration of the water through the repository and its transport to the Biosphere is indispensable for estimating the long term safety of the system. The evaluation of these phenomena is very complex and cannot be studied in the laboratory, since the physical (1 km^3) and temporal (0.1–1 My) scales involved are too great (Ménager *et al.*, 1992).

Rock salt formations, either bedded or domal, are currently considered suitable host-rock media for the disposal of high-level radioactive waste. This is due to their low permeability, high thermal conductivity, plastic behaviour, and also to the long-term stability of underground storage facilities built in rock salt (IAEA, 1977). Rock salt mines are considered to be dry when compared to other types of mines. Although many of them have been flooded by groundwater in the past, this problem could be overcome by the use of proper engineering barriers such as backfilling and construction of sealing structures (e.g. bulkheads, dams and plugs) in both galleries and shafts during the closure of the repository (IAEA, 1991). However, this external source of water is not discussed in this paper.

Due to their genesis and mineralogical composition, salt formations always contain small amounts of water (Roedder, 1984) that is present as interstitial brine, in hydrated minerals and as intragranular fluid inclusions (Jockwer, 1981; Roedder and Bassett, 1981). The water, depending on its form of entrapment, responds differently to heating, and it is thus important to discern and quantify this form. The chemical composition of the brine (Andriambololona *et al.*, 1992), and particularly the amount present in rock salt are of considerable importance to the design and the safety assessment of radioactive waste repositories (Olander, 1982). This water could eventually migrate through the repository, as a result of the existing thermal and pressure gradients induced by the presence of heat generating wastes (Jenks, 1979), corroding the waste container and afterwards leaching the radionuclides present in the waste.

This paper discusses the results of a rock salt survey performed within the framework of the research and development activities on radioactive waste disposal in Spain. The purpose of this study is to quantify and discern the distribution of the different kinds of water

present in the rock salt formations. Data on brine composition have been recently forwarded by Ayora *et al.* (1994a, 1994b).

GEOLOGICAL SETTING

Five Spanish rock salt units have been tested in this study: halite from the lower salt unit and halite interbedded in the potash seam of the Cardona Fm. (Upper Eocene, Catalonia sector), halite from the Zaragoza Fm. (Lower Miocene), halite from the lower salt unit of the Guendulain Fm. (Upper Eocene, Navarra sector) and diapiric rock salt from northern and southeastern Spain (Upper Triassic). Their location is shown in Fig. 1.

The Cardona Fm. and its equivalent saline formation of Navarra (Guendulain Fm.), were deposited during the Upper Eocene in a narrow and elongated marine evaporite basin, which extends from Navarra in the west, to Catalonia in the east, over more than 300 km. The saline formation is located between anoxic marine marls and red continental (alluvial and lacustrine) sediments. The saline body, which reaches a thickness of 300 m, has been divided into a lower salt unit, a potash seam and an upper salt unit (Busquets *et al.*, 1985).

The halite of the Zaragoza Fm. consists of a 100-m thick halitic unit belonging to a 700-m thick evaporitic formation. The salt corresponds to the inner part of a 100-km wide playa-lake system developed in the Lower Miocene at the centre of the Ebro Basin (Ortí and Pueyo, 1977).

Diapiric Triassic rock salt is extensively represented in southeastern (eight diapirs) and northern Spain (seventeen diapirs) covering an area of 2000 and 9000 km^2, respectively. Diapirs from southeastern Spain are formed by Upper Triassic salts (Rios, 1963). Here, two halitic units approximately 100-m thick are separated by a 250-m thick clay unit (Castillo-Herrador, 1974). Due to the arid climate of the area, rock salt crops out at the surface to frequently form positive relief. The diapirs from northern Spain consist of a thick halite unit (ranging between tens of metres and 8000 m) with minor intercalated clay, anhydrite, dolomite and volcanics (Serrano *et al.*, 1989). Diapirs crop out at the surface but, because of dissolution, salt has been cut only in oil exploration drillholes.

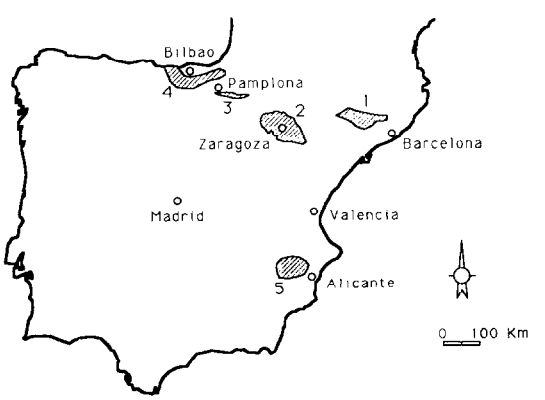

Fig. 1. Simplified map showing the location of the studied salt formations. 1 = Cardona Fm., 2 = Zaragoza Fm., 3 = Guendulain Fm., 4 = Triassic diapirs from northern Spain, 5 = Triassic diapirs from southeastern Spain.

EXPERIMENTAL PROCEDURES

Sampling

Rock salt from the Cardona Fm. was collected at the Sallent-Balsareny mine (Catalonia), whilst halite of the Zaragoza Fm. comes from the Remolinos mines (Zaragoza area), rock salt from the Guendulain Fm. has been obtained in the Javier area (Navarra), and diapiric rock salt comes from the diapirs of Alloz, Maestu, Iza, Estella, Aitzgorri (northern Spain) and Pinoso (southeastern Spain).

Most of the samples studied were test cores (76 mm diameter) obtained using saturated magnesian brine (when the boreholes began at the surface) or air (in mine boreholes) as drilling fluid. Otherwise, sampling was carried out by taking hand samples of approximately 500 g from salt mines. In order to avoid bias in the sampling procedure, random samples were taken at regular intervals for each rock selected.

Each rock type was sampled as extensively as possible to ensure statistical representivity. Sampling was performed in relatively pure salt beds, neglecting mudstone interbeds which are common in rock salt formations. These interbeds could be preferential pathways for brine (Hwang *et al.*, 1989) and should be avoided in the vicinity of the repository.

Analytical techniques

After the sampling stage, in order to prevent their hydration, samples were immediately stored in a low humidity room (relative humidity less than 35%). After crushing to a maximum size of approximately 1 cm, each samples was divided into two aliquots. The first was used for analysis of the water content, and the second milled for mineralogical and chemical analysis. The endpieces of the cores, or of hand samples, were stored and later used to obtain thin sections for petrographical purposes. All sample preparation was performed in the low humidity room.

Water content was analysed by thermogravimetry, since this technique allows the quantity and the types of water present in the rock salt to be discerned (De las Cuevas and Pueyo, 1991). 10 g of salt was taken from the corresponding aliquot and manually ground in a mortar to a grain size of 2 to 3 mm to overcome some hazards such as adsorption of water and the destruction of fluid inclusions. In this way the surface/volume ratio in the sample itself has been reduced, minimizing water adsorption from the atmosphere as well as preserving the majority of fluid inclusions. Several pieces of the crushed salt were hand picked to produce a 1 g sample (maximum capacity of the crucible) and taken for analysis. The working conditions are as follows: a temperature interval from 20 to 450°C, heating rate of 5°C/min and atmosphere of argon (argon flux: 2 l/h). Inside the thermoanalyser the crucible was covered with a double cap of platinum in order to avoid sample ejection due to fluid inclusion decrepitation. In addition, since water content values are very low, to overcome the buoyancy effect (apparent weight gain) due to purge gas buoyancy and/or convection currents

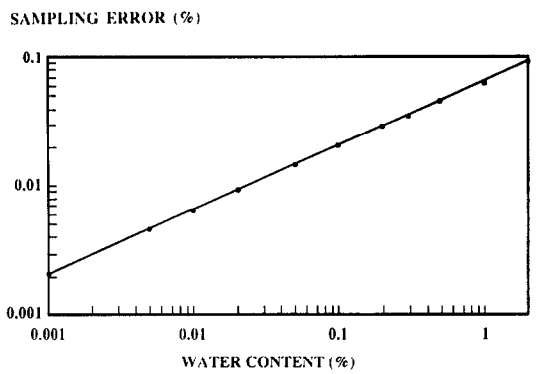

Fig. 2. Relationship between sampling error (95% level of confidence) and water content in rock salt.

inside the furnace, the experimental thermograms were subtracted to a blank (determined experimentally with an inert sample, under identical conditions as those of the samples). Precision of the thermogravimetrical analysis is 0.005%. The maximum temperature selected was 450°C, since from previous studies (Liptay, 1971; Jockwer, 1981) fluid inclusions finish their decrepitation at around 420°C, and clay minerals lose compositional water at temperatures between 400 and 700°C (Vallet, 1972). Under these working conditions, the characteristic temperatures for specific water-losses of the most common hydrated minerals present in rock salt are: between 80 and 130°C for gypsum and carnallite, 230 to 280°C for polyhalite and 350 to 390°C for kieserite. The intergranular brine liberates gradually until approximately 130°C whilst fluid inclusions decrepitate at higher temperatures, from 300 to 420°C.

Reproducibility of the thermogravimetrical analyses were performed by estimating the sampling error using Gy's equation after taking into account all the subsampling stages (Gy, 1979). The sampling error expressed in terms of standard deviation S equals

$$S^2 = \frac{C \cdot d^3}{M}$$

where M is the mass of sample (in g),
d, the diameter of the largest piece sampled (in cm),
C, a sampling constant.

The sampling constant, C, is a compound of various factors, such that

$$C = fgl(1 - a)[1.2(1 - a) + 2.2a]/a$$

where f is the shape factor (= 0.5),
g, the particle size distribution factor (= 0.5),
a, the water content (weight fraction),
l, the liberation factor (= 0.05 for d = 1, = 0.13 for d = 0.2).

In this case and due to a two-step subsampling procedure the total error S_t equals

$$S_t^2 = S_1^2 + S_2^2$$

Figure 2 displays the relationship between the water content and the sampling error, working with a confidence level of 95% (1.96 S_t). From this figure it can be deduced that for samples with 1.0% weight in water the error lies in ±0.07%, samples with 0.3% have an error of ±0.04, and samples with 0.01% show an error of ±0.008%. Errors have been checked by controlling in some samples the difference between the routine value and a duplicate. In the studied cases the difference of both values was inside the estimation error.

With regards to the mineralogical characterization, the mineral phases were identified by X-ray diffraction and their abundance computed from chemical analysis. Chlorides were determined volumetrically (Mohr method), sulphates determined by ICP-AES, and the insoluble fraction calculated gravimetrically (Huertas *et al.*, 1992). Finally, the petrographical characteristics were determined macroscopically and through thin section studies using a transmitted light polarizing microscope.

RESULTS

Description of the starting material

The lower salt unit of the Cardona Fm. is made up of massive, coarse grained (up to 1 cm) salt, with two main macroscopical facies: white salt (free of visible mineral impurities) and dark salt. The major mineral impurities are anhydrite (6.1% on average) and clays (0.5%). Microscopic observations reveal two halitic textures: cloudy halite (as big hopper crystals) rich in fluid inclusions (10 to 100 μm in size), and clear halite.

Salt of the potash seam of the Cardona Fm. is banded (each band 4-cm thick on average), fine grained (<1 mm), orange in colour, and with thin interbeds of clay (1-mm thick). The major accessory minerals are polyhalite (2.9% on average) and clay minerals (1.5%). Minor amounts of anhydrite and carnallite can also be detected. Two halitic textures are found: cloudy halite (as hopper crystals) and clear halite. The size of the fluid inclusions is less than 20 μm.

Salt of the Zaragoza Fm. is banded, coarse grained (up to 1 cm), with thin interbeds of clay (1-mm thick) and associated centimetre size anhydrite nodules. Two main macroscopical facies coexist: white salt free of impurities, and dark salt. The main impurities consist of anhydrite (1.4% on average) and clay minerals (0.4%). Halite has two textures: cloudy halite (with chevron structures and fluid inclusions ranging between 10 and 100 μm) and clear halite.

Although the lower salt unit of the Guendulain Fm. shows, in general, features similar to its equivalent in the Cardona Fm., the studied samples (from boreholes close to Pyrenean thrust sheets) consisted of brecciated salt made up of halite pebbles (up to 6 cm) in a halitic matrix (between 0.5 and 1 cm). Two macroscopical facies, white and dark salt, are present. The major accessory minerals are anhydrite (1.7% on average) and clays (1.2%). Occasionally, minor amounts of polyhalite can also be detected. Clear halite texture is dominant, the cloudy halite texture being subordinate, with fluid inclusions 10 to 50 μm in size.

Triassic diapiric salt is usually brecciated (each fragment 2–3 cm in size) showing a halitic matrix (between 2 and 5 mm) and, in many cases, foliation. It also contains a large amount of sulphatic minerals (essentially anhydrite) and clay. In some cases minor amounts of polyhalite and/or gypsum can also be found. Microscopy reveals a strong predominance of

Table 1. Main microstructural features and average mineralogical composition of the studied rock salt types

Salt formation	Lower S.U. Cardona Fm.	Lower S.U. Guendulain Fm.	Potash seam Cardona Fm.	Salt of Zaragoza Fm.	Spanish Triassic diapiric salt
Main structure	Massive. Broadly banded	Massive. Broadly banded or brecciated (<6 cm size)	Well banded (salt, 4 cm thick; clay, 1 mm thick)	Banded (clay 1 mm thick)	Brecciated (~foliated)
Grain size	Coarse grained <1 cm approx.	Coarse (0.5–1 cm) [pebbles <6 cm]	Fine grained <1 mm	Coarse grained <1 cm thick	Coarse grained (3 cm to 2 mm)
Colour of rock salt	White and grey with some reddish	White and grey	Orange	White and grey. Mainly white	Variable (grey, white, red or yellow)
Halite textures	Clear and cloudy (big hoppers) halite	Clear and cloudy (big hoppers) halite	Clear and cloudy (small hoppers) halite	Clear and cloudy (chevron) halite	Mainly clear halite
Size of fluid incl.	10–100 μm	10–50 μm	<20 μm	10–100 μm	<20 μm
Major accessory mins.	6.1% anhydrite 0.5% clays	1.7% anhydrite 1.2% clays some polyhalite	2.9% polyhalite 1.5% clays	1.4% anhydrite 0.4% clays	Large amount of sulphates (anyhydrite) and clays (some polyhalite and gypsum)
Textures in sulphates	Free crystals, or clusters	Free crystals, or clusters	Free crystals, or clusters	Free crystals and nodules	Free crystals, clusters and nodules

clear halite. The size of the fluid inclusions is less than 20 μm.

A summary of the main mineralogical and petrographical features of the rock salt types are given in Table 1.

Water content

Rock salt from the Lower Salt Units of the Cardona Fm. and Guendulain Fm., and the Zaragoza Fm. exhibit three mass losses (Fig. 3). A first loss from ambient temperature to 120°C is related to intergranular water, a second between 300 and 350°C, due to the decrepitation of large fluid inclusions (100 to 30 μm diameter), and a third which happens at 400°C upwards, related to the decrepitation of small fluid inclusions (<30 μm). Rock salt of the potash seam of the Cardona Fm. also exhibits three mass losses. The first loss is due to intergranular water, a second between 250 and 280°C related to the dehydration of polyhalite, and a third linked to the decrepitation of small fluid inclusions. Diapiric Triassic rock salt shows two mass losses related to intergranular water and decrepitation of small fluid inclusions.

Water contents for the studied samples (n = 240) are given in Table 2 for each unit. The data on water content have been expressed as total water as well as separated as intergranular water, and water related to fluid inclusions. The statistical parameters of the water content have been summarized in Table 3 for each rock type, and displayed as histograms in Fig. 4. The main feature of these data is that the water content usually shows a lognormal distribution. In three rock types (Lower salt units of the Cardona Fm. and Guendulain Fm., and the halite of the Zaragoza Fm.), water is mainly present as free brine. In contrast, in the samples from the halite of the potash

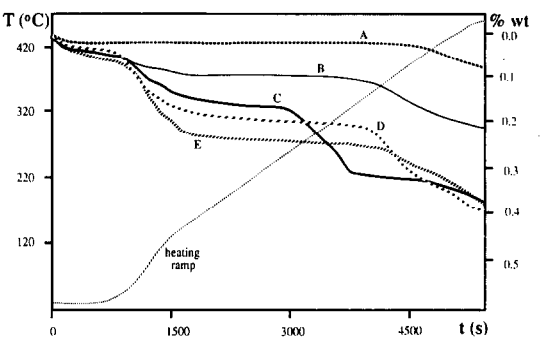

Fig. 3. Composite thermogram of representative samples of the five studied rock salt types. Thermogram A (- - -) belongs to Triassic diapiric rock salt and exhibits two mass losses, the first below 100°C (intergranular water) and the second around 400°C (fluid inclusions <20 μm). Thermogram B (——) has been performed on halite of the Zaragoza Fm. and shows three mass losses. The first, due to intergranular water liberation, a second around 300°C (fluid inclusions between 100 and 30 μm) and a third around 400°C (fluid inclusions below 30 μm). Thermogram C (——) which belongs to halite interbedded in the potash seam of the Cardona Fm., also exhibits three mass losses. The first and the third are similar to those of thermogram B, whereas the second mass loss (around 250°C) is related to the dehydration of polyhalite. Finally, thermograms D and E (both ....) performed on samples of the Lower Salt Unit of Cardona and Guendulain Fms., respectively, show behaviour similar to thermogram B.

Table 2. Chemical and water content data (expressed as wt%) from the Lower Salt Unit (LSU) of the Cardona Fm., salt from the potash seam (SPS) of the Cardona Fm., Zaragoza Fm., Lower Salt Unit (LSU) of the Guendulain Fm. and rock salt of Triassic diapirs

	CODE	TW	INS	HAL	SULF	IG	FI
L.S.U. of the Cardona Fm.	41011	0.69	0.42	89.43	2.77	0.39	0.30
	41012	0.50	0.43	96.99	2.57	0.26	0.23
	41021	0.21	0.33	99.32	2.56	0.10	0.11
	41022	0.24	0.26	98.15	1.33	0.08	0.16
	41031	0.04	0.52	97.57	1.81	0.03	0.01
	41032	0.34	0.63	90.01	3.57	0.17	0.16
	41041	0.60	0.79	92.34	7.83	0.37	0.23
	41042	0.80	0.23	90.01	4.67	0.46	0.34
	41051	0.07	0.40	95.75	2.70	0.03	0.04
	41052	0.36	0.50	95.83	3.71	0.25	0.11
	41071	0.14	0.75	95.25	4.81	0.10	0.04
	41072	0.31	0.84	95.83	5.35	0.23	0.08
	41081	0.74	0.73	87.11	4.67	0.46	0.28
	41082	0.66	0.47	90.60	3.91	0.52	0.14
	41091	0.15	0.73	95.25	5.46	0.09	0.06
	41092	0.17	0.44	98.73	1.40	0.16	0.01
	41101	0.73	0.66	78.39	6.98	0.47	0.26
	41102	0.85	0.42	91.18	5.31	0.70	0.15
	41111	0.34	0.56	94.08	4.59	0.21	0.13
	41112	0.44	1.31	96.99	4.33	0.31	0.13
	41121	0.59	0.78	95.83	4.03	0.46	0.13
	41122	0.66	0.69	87.69	7.96	0.46	0.20
	41131	0.64	1.21	77.22	12.12	0.44	0.20
	41132	0.46	0.89	90.01	10.37	0.30	0.16
	41141	0.54	1.51	83.62	14.79	0.40	0.14
	41142	0.65	0.98	85.49	12.07	0.40	0.25
	41151	0.84	1.39	83.62	16.32	0.64	0.19
	41152	1.00	1.51	85.36	15.57	0.82	0.18
	41181	0.38	0.64	84.78	11.94	0.23	0.15
	41182	0.82	1.16	84.75	14.92	0.54	0.28
	41191	0.75	1.61	74.90	17.78	0.52	0.23
	41192	0.46	1.55	81.29	21.01	0.35	0.11
	41201	0.60	0.47	92.92	9.13	0.25	0.35
	41202	0.12	0.29	99.32	2.52	0.08	0.04
	41211	0.44	0.35	94.50	3.13	0.36	0.08
	41212	0.07	0.14	91.18	1.20	0.03	0.04
	41221	0.12	0.20	90.01	3.74	0.06	0.06
	41222	0.46	0.51	91.76	4.97	0.20	0.26
	41251	0.35	1.28	86.53	12.03	0.28	0.07
	41252	0.55	0.92	92.34	9.90	0.36	0.19
	41261	0.49	1.28	85.94	14.43	0.35	0.14
	41262	0.56	1.23	86.53	13.19	0.44	0.12
	41281	0.33	0.31	85.36	6.56	0.22	0.11
	41282	0.22	0.18	94.08	5.63	0.15	0.07
	41291	0.33	0.48	91.76	8.58	0.21	0.12
	41292	0.76	0.46	96.99	5.07	0.54	0.22
	41311	0.47	0.31	94.08	5.28	0.25	0.22
	41312	0.53	0.64	92.34	8.64	0.32	0.21
	41321	0.49	1.18	85.36	13.31	0.26	0.23
	41322	0.29	0.64	94.08	7.04	0.21	0.08
	42012	0.19	0.23	95.45	3.24	0.14	0.05
	42021	0.15	0.26	99.00	1.60	0.11	0.04
	42022	0.28	0.32	96.61	2.87	0.19	0.09
	42031	0.21	0.28	98.35	2.82	0.15	0.06
	42032	0.31	0.29	98.93	2.14	0.28	0.03
	42041	0.17	0.24	98.35	1.80	0.08	0.09
	42042	0.14	0.24	97.77	2.11	0.08	0.06
	42051	0.11	0.29	98.35	3.31	0.03	0.08
	42052	0.32	0.22	97.77	1.65	0.16	0.16
	42061	0.25	0.29	97.19	2.57	0.17	0.08
	42062	0.33	0.39	96.03	2.55	0.24	0.09
	42081	0.19	0.18	97.77	2.15	0.09	0.10
	42082	0.51	0.13	97.19	2.60	0.36	0.16
	42112	0.59	0.18	98.35	1.54	0.25	0.34
	42121	0.42	0.18	97.77	2.62	0.19	0.23
	42151	0.44	0.14	97.77	2.33	0.27	0.17
	42152	0.32	0.24	95.45	4.28	0.14	0.18
	42161	0.09	0.27	97.77	3.91	0.03	0.06
	42162	0.21	0.13	91.98	2.80	0.09	0.12
	42171	0.35	0.22	96.03	2.50	0.15	0.20
	42172	0.31	0.20	98.35	1.98	0.17	0.14
	42191	0.27	0.28	97.19	1.72	0.15	0.12
	42192	0.16	0.30	96.61	1.84	0.08	0.08
	42201	0.15	0.31	98.35	1.84	0.07	0.08
	42202	0.09	0.16	94.87	1.82	0.03	0.06
	42221	0.29	0.26	97.77	1.36	0.08	0.21
	42222	0.10	0.26	97.77	0.93	0.04	0.06
	42231	0.23	0.29	98.35	1.56	0.10	0.13
	42232	0.17	0.28	97.77	2.04	0.06	0.11
	42261	0.24	0.20	99.50	1.12	0.09	0.15
	42262	0.20	0.25	98.35	1.36	0.08	0.12
	42291	0.18	0.30	98.92	1.20	0.12	0.06
	42292	0.18	0.28	98.15	1.56	0.05	0.13
	42331	0.35	0.20	97.19	1.53	0.06	0.29
	42322	0.11	0.24	99.50	1.16	0.04	0.07
	42341	0.36	0.12	99.35	0.90	0.08	0.28
	42342	0.37	0.23	98.92	0.76	0.09	0.28
	42122	0.39	0.00	98.92	1.13	0.14	0.25
	11011	0.17	0.20	94.60	4.76	0.09	0.08
	11012	0.07	0.10	98.13	2.55	0.04	0.03
	11021	0.32	0.20	96.37	3.50	0.11	0.21
	11022	0.26	0.80	88.73	5.78	0.14	0.12
	11041	0.27	0.20	94.60	5.51	0.10	0.17
	11042	0.30	0.20	90.49	8.05	0.13	0.17
	11051	0.36	0.30	92.84	7.72	0.21	0.15
	11052	0.33	0.40	93.43	7.31	0.17	0.16
	11071	0.40	0.50	95.78	7.88	0.15	0.25
	11072	0.15	0.20	98.13	2.27	0.05	0.10
	11091	0.99	0.70	73.45	26.21	0.67	0.22
	11092	0.63	0.50	80.50	16.62	0.29	0.34
	11101	0.29	0.40	93.43	5.35	0.10	0.29
	11102	0.85	0.40	89.32	10.30	0.52	0.33
	11121	0.17	0.20	95.19	4.86	0.09	0.08
	11122	0.19	0.50	88.73	13.88	0.08	0.11
	11131	0.14	0.30	98.13	0.71	0.04	0.10
	11132	0.06	0.40	94.60	3.84	0.03	0.03
	11141	0.23	0.50	93.43	5.61	0.12	0.11
	11142	0.32	0.01	92.84	6.63	0.19	0.13
	11151	0.31	0.40	94.02	6.93	0.13	0.18
	11152	0.28	0.30	96.37	3.60	0.10	0.18
	11181	0.28	0.30	95.19	4.15	0.10	0.18
	11182	0.23	0.20	98.72	1.80	0.12	0.11
	11191	0.26	0.30	97.54	2.25	0.12	0.14
	11192	0.28	0.30	96.95	3.81	0.15	0.13
	11211	0.33	0.50	93.43	6.34	0.16	0.17
	11212	0.46	0.40	95.19	5.30	0.26	0.20
	11231	0.22	0.50	95.78	5.61	0.10	0.12
	11232	0.22	0.30	91.08	8.36	0.10	0.12
	11251	0.45	0.40	92.84	6.93	0.16	0.29
	11252	0.48	0.40	94.02	4.59	0.21	0.27
	11271	0.38	0.40	92.84	7.07	0.22	0.16
	11272	0.56	0.70	85.20	14.10	0.26	0.30
	11301	0.32	0.40	84.03	15.60	0.19	0.13
	11302	0.31	0.20	76.39	16.28	0.14	0.17
	11311	0.24	0.40	98.13	1.78	0.08	0.16
	11312	0.24	0.20	88.14	3.59	0.11	0.13
	11331	0.29	0.60	88.73	11.70	0.14	0.15
	11332	0.29	0.40	92.25	7.40	0.08	0.21
	11341	0.31	0.60	90.49	9.18	0.15	0.16
	11342	0.19	0.60	90.49	9.72	0.06	0.11
ZARAGOZA FM.	rem1	0.09	0.66	94.15	1.02	0.07	0.02
	rem2	0.20	0.56	80.29	3.00	0.06	0.14
	rem3	0.37	0.23	97.62	0.61	0.05	0.32
	rem4	0.25	0.22	99.35	1.00	0.04	0.21
	rem5	0.23	0.22	99.35	0.04	0.07	0.26
	rem6	0.35	0.19	94.73	1.07	0.08	0.27
	rem6-7	0.22	0.40	68.74	1.71	0.10	0.10
	rem7	0.39	0.26	97.62	0.37	0.10	0.29
	rem8	0.47	0.30	99.35	0.24	0.20	0.27
	rem9	0.38	0.36	95.89	0.76	0.13	0.25
	rem10	0.30	0.24	99.93	0.00	0.05	0.25
	rem10′	0.43	0.43	95.31	0.42	0.10	0.33
	rem11	0.28	0.32	99.93	0.45	0.05	0.23
	rem12	0.10	0.25	97.62	0.88	0.04	0.06
	rem13	0.27	0.25	95.89	0.00	0.02	0.25
	rem16	0.07	0.24	99.93	0.00	0.03	0.04
	rem17	0.10	0.16	98.20	0.00	0.04	0.06
	rem17′	0.13	0.20	93.00	0.00	0.06	0.07
	rem17″	0.15	0.15	99.93	1.77	0.09	0.06
	rem19	0.07	0.72	90.11	1.65	0.05	0.02
	rem20	0.26	0.34	99.93	1.47	0.17	0.09
	rem21	0.17	0.50	97.62	2.21	0.12	0.05
	rem22	0.21	0.98	94.15	2.96	0.12	0.09
	rem23	0.10	0.23	99.93	0.41	0.04	0.06
	rem24	0.11	0.43	92.42	4.53	0.05	0.06
	rem26	0.42	0.18	99.35	0.65	0.07	0.35
	rem27	0.08	0.27	99.35	0.46	0.03	0.00
	rem28	0.33	0.26	98.78	0.35	0.08	0.25
	rem29	0.23	2.59	85.49	4.23	0.05	0.18
	rem30	0.25	0.05	97.62	2.31	0.06	0.19
	rem31	0.15	0.26	97.62	4.77	0.05	0.10
	rem32	0.13	0.15	94.15	2.28	0.05	0.08
	rem33	0.18	0.05	99.35	0.93	0.04	0.14
	la real	0.18	0.20	98.78	0.11	0.11	0.07
S.P.S. of the Cardona Fm.	bis-1	0.54	0.96	94.10	4.94	0.20	0.05
	bis-2	0.52	2.64	93.66	3.70	0.24	0.10
	bis-3	0.40	2.28	94.62	3.10	0.18	0.07
	bis-4	0.10	0.98	98.18	0.84	0.04	0.01
	bis-5	1.02	1.37	96.60	2.03	0.16	0.15
	bis-6	0.23	2.16	95.31	2.53	0.07	0.02
	bis-7	0.10	0.55	98.62	0.83	0.04	0.01
	bis-8	0.04	0.39	99.11	0.50	0.01	0.01

Continued

Table 2. Continued

	CODE	TW	INS	HAL	SULF	IG	FI
	bis-9	0.05	0.77	98.73	0.50	0.01	0.01
	bis-10	0.38	0.62	94.78	4.60	0.04	0.07
	bis-11	0.07	1.21	98.19	0.60	0.03	0.01
	bis-12	0.29	0.74	95.85	3.41	0.08	0.02
	bis-13	0.07	1.16	98.34	0.50	0.03	0.01
	bis-14	0.24	0.27	98.56	1.17	0.14	0.03
	bis-15	0.09	3.02	96.11	0.87	0.04	0.01
	bis-16	0.07	2.56	96.68	0.76	0.02	0.01
	bis-17	1.86	3.27	78.87	17.86	0.10	0.10
N. SPAIN	g-1	0.04	4.87	82.45	12.68	0.04	0.00
Diapiric salts	g-2	0.05	3.49	91.64	4.87	0.05	0.00
	g-5	0.06	1.76	96.40	1.84	0.03	0.03
	g-10	0.07	14.86	62.41	22.73	0.04	0.03
	g-11	0.74	5.31	89.51	5.18	0.07	0.03
	g-12	2.58	9.87	81.54	8.59	0.39	0.01
	g-20	1.42	6.22	85.99	7.79	0.07	0.02
	g-21	0.14	2.18	96.97	0.85	0.09	0.01
	g-31	0.02	19.64	65.29	15.07	0.01	0.01
	g-32	0.09	6.39	83.56	10.05	0.07	0.02
	g-33	0.40	3.11	92.76	4.13	0.02	0.03
SE. SPAIN	p-1	0.13	0.56	97.20	2.24	0.03	0.10
Pinoso diapir	p-2	0.11	1.08	96.54	2.38	0.06	0.05
	p-3	3.50	27.31	36.42	36.27	0.30	0.01
	p-4	0.14	1.77	96.13	2.10	0.10	0.04
	p-5	0.27	2.47	93.66	3.87	0.12	0.15
L.S.U. of the	n-1	0.09	0.32	98.66	1.02	0.07	0.02
Guendulain	n-2	0.32	0.57	98.66	0.77	0.22	0.10
Fm.	n-3	0.38	0.33	97.32	2.35	0.09	0.16
	n-4	0.07	0.20	99.64	0.16	0.04	0.03
	n-5	0.70	5.79	86.05	8.16	0.12	0.05
	n-6	0.10	0.27	99.18	0.55	0.08	0.02
	n-7	0.39	0.83	97.20	1.97	0.20	0.19
	n-8	0.65	2.66	94.07	3.27	0.33	0.32

CODE	TW	INS	HAL	SULF	IG	FI
n-9	0.38	1.58	96.74	1.68	0.25	0.13
n-10	0.23	0.72	97.96	1.32	0.15	0.08
n-11	1.08	6.23	85.94	7.83	0.22	0.03
n-12	0.10	0.94	95.69	3.37	0.07	0.03
n-13	0.11	0.26	98.71	2.03	0.09	0.02
n-14	0.01	0.17	99.73	0.10	0.01	0.00
n-15	0.10	0.14	99.18	0.68	0.06	0.04
n-16	0.10	0.42	98.37	1.21	0.07	0.03
n-17	0.07	0.24	98.48	1.28	0.03	0.04
n-18	0.47	0.18	98.66	1.16	0.09	0.10
n-19	0.21	0.46	98.31	1.23	0.14	0.07
n-20	0.40	0.57	97.96	1.47	0.30	0.10
n-21	0.51	0.82	97.90	1.27	0.40	0.11
n-22	0.18	0.36	98.14	1.50	0.15	0.03
n-23	0.08	0.61	97.50	1.89	0.03	0.05
n-24	0.85	0.47	98.02	1.51	0.62	0.23
n-25	0.25	0.64	99.06	0.30	0.17	0.08
n-26	1.08	0.40	98.08	1.52	0.40	0.40
n-27	0.37	0.26	98.37	1.37	0.17	0.20
n-28	0.06	0.23	99.67	0.10	0.05	0.01
n-29	0.11	0.07	99.83	0.10	0.08	0.03
n-30	0.20	0.41	99.12	0.47	0.14	0.06
n-31	0.41	1.95	95.56	2.49	0.18	0.10
n-32	0.37	0.77	96.96	2.27	0.28	0.11
n-33	0.37	1.19	96.50	2.31	0.20	0.17
n-34	0.36	0.24	99.00	0.76	0.23	0.13
n-35	0.01	0.12	99.78	0.10	0.01	0.00
n-36	0.46	0.65	98.13	1.22	0.28	0.18
n-37	0.17	0.77	98.01	1.22	0.07	0.10
n-38	0.55	6.67	92.01	1.32	0.33	0.22
n-39	0.54	4.92	89.62	5.46	0.12	0.03
n-40	0.02	0.28	99.40	0.32	0.02	0.00
n-41	1.38	2.14	95.85	2.01	0.94	0.30
n-42	0.53	1.35	97.78	0.87	0.31	0.22
n-43	0.63	1.75	95.62	2.63	0.15	0.05

CODE: Sample code.
TW: Total water content.
INS: Content in water-insoluble minerals.
HAL: Halite content.
SULF: Sulfatic mineral content.
IG: Intergranular water content.
FI: Fluid inclusions water content.

Table 3. Water content statistical parameters (range, average and standard deviation) of the studied rock salt units. Data have been grouped regarding their contents in total water, free water, intergranular water, water present in fluid inclusions and compositional water in hydrated minerals

Salt formation	Lower S.U. Cardona Fm.	Lower S.U. Guendulain Fm.	Potash seam Cardona Fm.	Salt of Zaragoza Fm.	Spanish Triassic diapiric salt
Total amount of water	0.04–1.00% $\bar{x} = 0.32\%$ $s = 0.20$	0.01–1.38% $\bar{x} = 0.35\%$ $s = 0.31$	0.04–1.86% $\bar{x} = 0.35\%$ $s = 0.46$	0.07–0.47% $\bar{x} = 0.23\%$ $s = 0.11$	0.04–3.50% $\bar{x} = 0.61\%$ $s = 1.03$
Free water	0.04–1.00% $\bar{x} = 0.32\%$ $s = 0.20$	0.01–1.24% $\bar{x} = 0.29\%$ $s = 0.25$	0.02–0.38% $\bar{x} = 0.12\%$ $s = 0.10$	0.07–0.47% $\bar{x} = 0.23\%$ $s = 0.11$	0.04–0.40% $\bar{x} = 0.16\%$ $s = 0.13$
Intergranular brines	0.03–0.82% $\bar{x} = 0.18\%$ $s = 0.14$	0.01–0.94% $\bar{x} = 0.18\%$ $s = 0.17$	0.01–0.24% $\bar{x} = 0.08\%$ $s = 0.07$	0.02–0.18% $\bar{x} = 0.07\%$ $s = 0.04$	0.01–0.39% $\bar{x} = 0.09\%$ $s = 0.10$
Fluid inclusion brines	0.01–0.35% $\bar{x} = 0.14\%$ $s = 0.08$	0.00–0.40% $\bar{x} = 0.10\%$ $s = 0.09$	0.01–0.12% $\bar{x} = 0.04\%$ $s = 0.04$	0.01–0.35% $\bar{x} = 0.16\%$ $s = 0.10$	0.00–0.15% $\bar{x} = 0.03\%$ $s = 0.04$
Compositional water	Not detected	0.00–0.83% $\bar{x} = 0.07\%$ $s = 0.17$	0.02–1.66% $\bar{x} = 0.23\%$ $s = 0.39$	Not detected	0.00–3.19% $\bar{x} = 0.51\%$ $s = 0.94$

seam of the Cardona Fm. and the diapiric Triassic rock salt, water is basically present in the form of hydrated minerals, the contribution of free brine being almost negligible. In these cases, small amounts of polyhalite, carnallite, gypsum and/or kaolinite strongly increase the amount of water present in the rock salt.

Analysis of variance was combined with the free brine content data to check if the differences in the amount of brine are significant. The results of the analysis enabled us to distinguish between water-rich rock salt (around 0.3% on average; as found for the lower salt units of the Cardona Fm. and the Guendulain Fm.), intermediate water-rich rock salt (around 0.2% on average; as in the halite of the Zaragoza Fm.) and water-poor rock salt (around 0.1% on average; the halite of the potash seam of the Cardona Fm. and the diapiric Triassic rock salt).

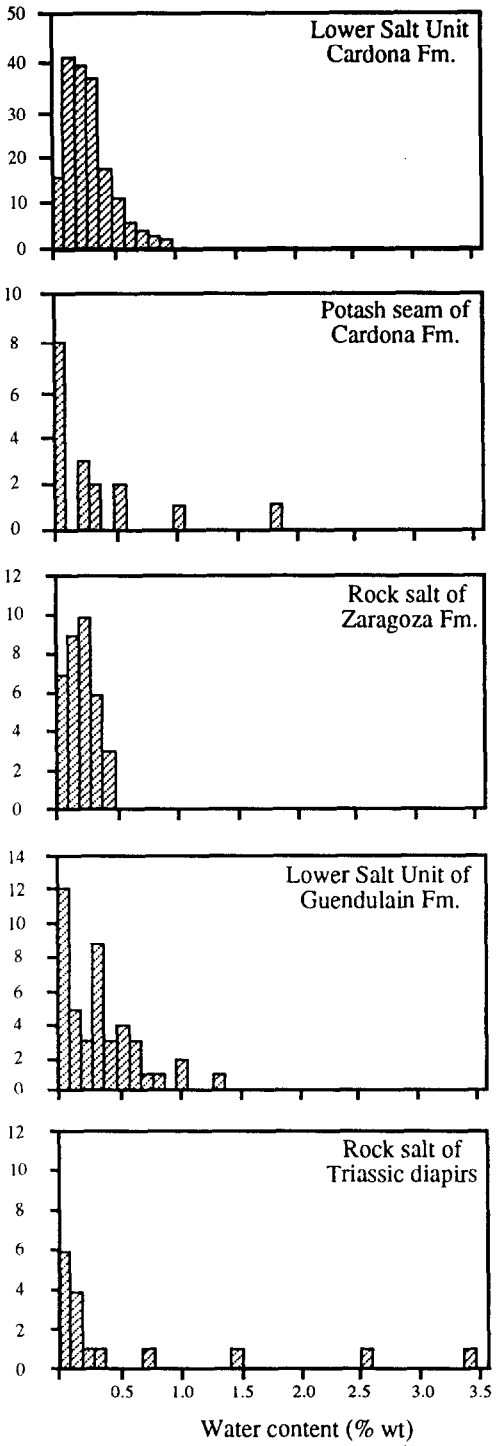

Fig. 4. Histograms of the total water content in rock salt of the Lower Salt Unit of the Cardona Fm., salt of the potash seam of the Cardona Fm., rock salt of Zaragoza Fm., Lower Salt Unit of the Guendulain Fm. and rock salt of Triassic diapirs.

Influence of the mineralogical composition on the water content of rock salt

In order to determine if there is a relation between the water content and the mineralogical composition, principal component analysis (PCA) using the correlation matrix was performed for each rock type. The input variables were the contents of halite, sulphatic minerals, clay minerals, total water, intergranular water and fluid inclusion water. The aim of PCA is to attempt these multivariate data sets using as few factors as possible. The results of the analysis are listed in Table 4.

For all cases, 80% or more of the total variance can be described in terms of one or two components. In the case of bedded salt, the amount of water is related to mineralogical composition. Intergranular water shares positive loadings with sulphatic and clay minerals content, whereas halite shows a negative behaviour. The amount of water in the form of fluid inclusions is related to intermediate loadings of halite content. In contrast, for diapiric salt, the first component (53% of total variance) explains the amount of water related to the mineralogical composition. The second component (26% of total variance) essentially weights the preservation of original textures and intergranular water during halokinesis.

DISCUSSION

The five studied rock salt units show a huge variation with regard to their mineralogy, texture, sedimentology and internal structure. A first division has been made based upon their internal structure as diapiric or bedded salt.

The water content in the Spanish Triassic diapiric salt is similar to those of the German Permian diapiric salt (Jockwer, 1981). In Permian salt, water is mainly related to the presence of polyhalite, fluid inclusions being scarce. Original textures of the salt have been wiped out due to the effect of diapirism. Rock salt from the diapirs of northern Spain (Table 2) have a transparent halitic texture, and their quantity of fluid inclusions is very low (0.01–0.03% weight). In contrast, rock salt of the Pinoso diapir [southeastern Spain] (Table 2) exhibits a higher variability in their fluid inclusion content (0.01–0.15% weight) that correlates with sedimentological and petrographical features (preservation of original banding and halitic textures [Ortí and Pueyo, 1983]).

Regarding the bedded salt, three salt units (lower salt unit of the Cardona Fm., halite of the Zaragoza Fm. and halite of the potash seam of the Cardona Fm.) show abundant and well preserved primary structures such as *hoppers* or *chevrons* (see Table 1), the size and amount of fluid inclusions being higher in the two first units than in the third one. This is mainly due to the fine grain size of the rock salt in the potash seams which hinders the development of large inclusions. The amount of fluid inclusions is also low in the lower salt unit of the Guendulain Fm. that correlates with the scarcity of primary structures because the rock salt formation was strongly affected during the emplacement of the Pyrenean thrust sheets. In

Table 4. Loadings of the relevant eigenvectors (Components) obtained by Principal Component Analysis from the Lower Salt Unit of the Cardona Fm., salt from the potash seam of the Cardona Fm., rock salt of Zaragoza Fm., Lower Salt Unit of the Guendulain Fm. and rock salt of Triassic diapirs. TW = total water, IG = intergranular brine, SULF = sulphatic minerals, HAL = halite, INS = insoluble fraction (mainly clay minerals), FI = brine present in fluid inclusions

		Lower S.U. Cardona Fm.	Salt of the potash seam Cardona Fm.	Salt of the Zaragoza Fm.	Lower S.U. Guendulain Fm.	Salt of Triassic diapirs
Component 1	TW	0.89	0.98	0.85	0.87	0.46
	IG	0.87	0.92	0.39	0.60	0.41
	SULF	0.84	0.91	−0.62	0.79	0.87
	HAL	−0.84	−0.93	0.46	−0.87	−0.89
	INS	0.76	0.59	−0.43	0.84	0.92
	FI	0.56	0.77	0.82	0.50	−0.61
Component 2	TW	0.38		0.49	0.40	0.80
	IG	0.16		0.46	0.72	0.82
	SULF	−0.35		0.51	−0.51	−0.26
	HAL	0.29		−0.59	0.48	0.09
	INS	−0.42		−0.69	−0.40	−0.23
	FI	0.69		0.34	0.76	0.30

general, the amount of intergranular water is enhanced with the presence of mineral impurities, suggesting an increase in porosity of anhydrite-clay-bearing rock salt leading to a better entrapment of brine. This effect can be well observed in rock salt of the Zaragoza Fm. (Tables 2 and 3).

A test of the differential distribution of water between clear and cloudy halite has been performed in several samples of the lower salt unit of the Cardona Fm. where both textures can be easily separated under a binocular lens. Some specimens of both halite types were hand picked and thermogravimetrical analysis for each texture was performed (Fig. 5). Whilst clear halite contains only intergranular water (around 0.30%), cloudy halite has its water mainly in the form of fluid inclusions (both large and small size), the intergranular water content being very similar to that of clear halite.

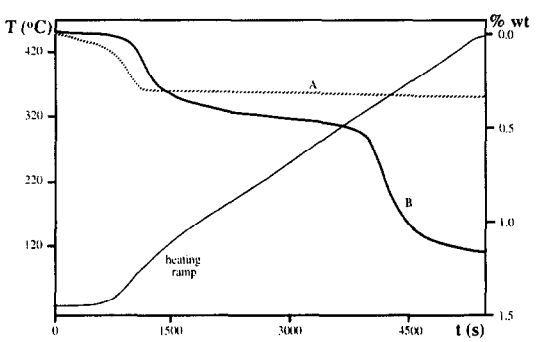

Fig. 5. Composite thermogram of the two major halitic textures present in the studied samples. Thermogram A (– – –) belongs to clear halite and exhibits one mass loss related to intergranular brine. Thermogram B (——) belonging to cloudy halite, exhibits two mass losses. The first is related to intergranular water and the second (major mass loss) to the decrepitation of fluid inclusions.

Implications for radioactive waste disposal

High-level radioactive waste acts as a heat and radiation source when it is emplaced in salt formations. The production of heat gives rise to a temporary local heating (the first 10 y) and a long lasting heating of the surrounding rock salt (about the first 1000 y). The high temperatures are responsible for some thermomechanical perturbations as well as gas and brine migration in the near-field of repositories (De las Cuevas *et al.*, in press). Irradiation causes radiation damage in the rock salt, as well as some generation of radiolytical gas (Akram *et al.*, 1992).

The main concern of the presence of brine in the safety of high level waste repositories in salt is its migration through the vault. Two possible mechanisms for brine migration can take place: fluid inclusion movement through halite crystals and vapour movement through pore space. Fluid inclusions of saturated brine can migrate through salt grains following temperature gradients. In the case where a gaseous phase is also present inside the fluid inclusions, these migrate in the opposite direction of the temperature gradient. For temperature gradients between 0.2 and 1°C/cm (Pigford, 1982) only inclusions larger than 100 μm move through the salt grains until they reach a grain boundary being incorporated into the intergranular brine. Vapour migration is the form of motion of water present in the pore space, or the water formed from hydrated minerals, at high temperature (Rothfuchs, 1986), motion that is pressure and temperature dependent. Preliminary porosimetric analysis in samples from the lower salt unit of the Cardona Fm. show pore size diameters between 10 and 30 nm (De las Cuevas, 1992). This means that Knudsen diffusion may be the leading mechanism of mass transfer (100 nm is the smaller pore diameter for advective flux [Schlich, 1986]).

Small amounts of hydrated minerals (like polyhalite, gypsum and/or carnallite) can substantially increase the amount of total water present in the rock (as happens with the halite of the potash seam of the Cardona Fm. and the diapiric Triassic rock salt in the cases studied [see Table 3]). In a real repository placed in a salt formation, with temperatures lower than 200°C, only carnallite and/or gypsum in the vicinity of the disposal horizons can dehydrate, and hence form an additional source of brine (Jockwer, 1981; De las Cuevas, 1992). The presence of polyhalite is not so critical since, as has been proved from *in situ* heating tests (Schlich and Jockwer, 1985), it dehydrates at temperatures higher than 230°C.

Although the radiation damage is restricted to the first metre from the contact with the waste containers (Schulze, 1986), it should be taken into account in repository safety assessments. Gamma radiation damages the NaCl lattice by developing defects such as F and H centres. These can accumulate upon prolonged exposure to radiation, tending to form molecular chlorine and favouring the reaction of F-centre with Na^+, which gives metallic sodium particles of colloidal size (Jain and Lidiard, 1977). The energy associated with the creation of these defects is fixed in the NaCl crystals as stored energy. A possible hazard bound to hypothetical reactions between metallic sodium with chlorine would be the sudden release of all the energy stored in the crystal lattice, once the concentration of colloidal sodium reaches the percolation value. This release could raise the local temperature around the emplacement (Mönig *et al.*, 1990).

The presence of small amounts of intergranular water permit fluid-assisted recrystallization which may reduce radiation damage in irradiated rock salt (García Celma *et al.*, 1988). This consists in the solution, transport and reprecipitation of halite (free of damage), and proceeds if at least 0.05% of intergranular water is present at the grain boundary voids (pore space), even if water is at the vapour state (García Celma *et al.*, 1993). However, fluid-assisted recrystallization can be hindered by the presence of mineral impurities in the rock salt acting as physical barriers (De las Cuevas *et al.*, 1993).

The contact between metallic sodium and brine during the fluid-assisted recrystallization could be responsible for the generation of hydrogen following the reaction (Jenks *et al.*, 1975)

$$2Na^0 + 2H_2O = H_2 + 2Na^+ + 2OH^-$$

However, the amount of water consumed in the reaction as well as due to direct radiolysis of water, can be considered negligible, as has been proved in laboratory experiments (De las Cuevas *et al.*, 1993) and *in situ* tests (Jenks, 1979; Rothfuchs, 1986). In addition, the reprecipitated halite crystals (radiation damage free) trap, as gas inclusions, a significant amount of the hydrogen produced in the reaction (García Celma *et al.*, 1988).

The presence of water should also be considered in the design of the repository, because it lowers the mechanical strength of rock salt. Under repository conditions (long-term deformation and low-strain rate) the prevailing deformation mechanism involves fluid-assisted recrystallization and diffusive mass-transfer creep caused by the high solubility of halite and by rapid diffusion of the constituent ions (Urai, 1983). This effect, observed in rock salt bearing small amounts of intergranular water (0.05%), can be faster if large amounts of intergranular water (0.25–0.50%) are present (Spiers *et al.*, 1986).

CONCLUDING REMARKS

This study shows clear differences in the amount of water and form of water entrapment present in the samples of the studied salt formations, where water can be present basically in the form of intergranular brine (lower salt units of Cardona Fm. and Guendulain Fm.), as intergranular fluid inclusions (Zaragoza Fm.) or as compositional water in hydrated minerals (interbedded halite in the potash seam of the Cardona Fm. and diapiric Triassic rock salt).

After having covered a wide range of Spanish rock salt examples of different geological features, and considering their free water content, ancient salt formations can be considered as water-poor (around 0.1%), intermediate water-rich (around 0.2%) and water-rich (higher than 0.3%). Small amounts of hydrated minerals (such as polyhalite, gypsum and/or carnallite) can notably increase the amount of total water present in the rock.

The amount of intergranular brine in bedded salt formations rises with the increase in the mineral impurity content. Petrographical data show that the amount of water present in fluid inclusions is related to the halitic texture and/or the grain size of the rock salt. Cloudy halite and coarse grained rock salt present, in general, more fluid inclusion-bounded water than clear halite or fine grained rock salt. In diapiric rock salt, stresses favour the migration of interstitial brine and the progressive destruction of original textures rich in fluid inclusions, decreasing the total amount of water. However, further work on diapiric rock salt remains to be done in order to obtain more data on the relationship between the amount of intergranular brine and the degree of deformation during halokinesis.

Our results suggest that the mineralogical content plays the most important role in retaining fluids in the rock salt during diagenetic and/or halokinetic processes. In the context of the use of salt formations as radioactive waste disposal sites, and besides other considerations such as mining of the salt bodies, rock salt with a purity higher than 95% in halite, without hydrated minerals (particularly gypsum and carnal-

lite), and with small-sized fluid inclusions, seems to be the most suitable to host radioactive wastes. In addition, the consequences of brine migration could be minimized by keeping as low as reasonably achievable the maximum temperatures in the vault.

Acknowledgements—The authors express their gratitude to the National Waste Management Company of Spain (ENRESA) for the financial support of this work. Part of it was conducted under the auspices of the Programme on Radioactive Waste Management of the Commission of the European Communities [Contract CEC FI-1W-0235-E (TT)]. Special thanks are given to the Potasas del Llobregat, Posusa, Remosal and Union Salinera de España mining companies for their assistance during the sampling stage, and to Repsol Exploracion for submitting samples from oil exploration boreholes. We also wish to thank J. M. Grosso for performing chemical analyses. The comments and criticism of M. Pagel, N. Akram and N. Jockwer have greatly improved the final version of the manuscript.

Editorial handling: Dr J. C. Petit.

REFERENCES

Akram N., Gaudez M. T., Toulhoat P., Mönig J. and Palut J. M. (1992) Multi-parameter study of gas generation induced by radiolysis of rocksalt in radioactive waste repositories. In *Proceedings of the Workshop on Gas Generation and Release from Radioactive Waste Repositories*. Aix-en-Provence, NEA-OCDE, 130–140.

Andriambololona Z., Godon N. and Vernaz E. (1992) R7T7 nuclear glass alteration in a saline medium: in situ experiments in the WIPP Project. *Appl. Geochem. Suppl.* **1**, 23–32.

Ayora C., García Veigas J. and Pueyo J. J. (1994a) X-ray microanalysis of fluid inclusions and its importance to the geochemical modeling of evaporite basins. *Geochim. Cosmochim. Acta* **58**, 43–55.

Ayora C., García Veigas J. and Pueyo J. J. (1994b) The chemical and hydrological evolution of an ancient potash-forming evaporite basin as constrained by mineral sequence, fluid inclusion composition, and numerical simulation. *Geochim. Cosmochim. Acta* **58**, 3379–3394.

Busquets P., Ortí F., Pueyo J. J., Riba O., Rosell L., Saez A., Salas R. and Taberner C. (1985) Evaporite deposition and diagenesis in the Saline (Potash) Catalan Basin, Upper Eocene. *VI European Regional Meeting IAS*, Lleida, Excursion Guide-book: 11–59.

Castillo-Herrador F. (1974) La Trias évaporitique des bassins de la Vallée de l'Ebre et de Cuenca. *Bull. Soc. Geol. Fr.* **16**, 666–676.

De las Cuevas C. (1992) Análisis del contenido en agua en formaciones salinas. Su aplicación al almacenamiento de residuos radiactivos. Ph.D. Thesis, Univ. Barcelona, 175 pp.

De las Cuevas C. and Pueyo J. J. (1991) Caracterización y cuantificación termogravimétrica de los diferentes tipos de agua presentes en formaciones salinas. *Bol. Soc. Esp. Min.* **14**, 15–21.

De las Cuevas C., Miralles L., Teixidor P., García Veigas J., Dies X., Ortega X. and Pueyo J. J. (1993) *Spanish Participation in the HAW Project: Laboratory Investigations on Gamma Irradiations Effects in Rock Salt*. Publ. Tecn. 04/93 ENRESA, 85 pp.

De las Cuevas C., Teixidor P. and Miralles L. (in press) Potential gas generation in rock salt repositories. In *Project on Effects of Gas in Underground Storage Facilities for Radioactive Waste (Pegasus Project)*, B. Haijtink and T. McMenamin (Eds). To be published in Nuclear Science and Technology EUR Series, 15 pp.

García Celma A., Urai J. L. and Spiers C. J. (1988) *A Laboratory Investigation into the Interaction of Recrystallization and Radiation Damage Effects in Polycrystalline Salt Rocks*. Nuclear Science and Technology EUR 11849 EN, 125 pp.

García Celma A., de las Cuevas C., Teixidor P., Miralles L. and Donker H. (1993) On the possible continuous operation of an intergranular process of radiation damage anneal in rock salt repositories. In *Geological Disposal of Spent Fuel and High Level and Alpha Bearing Wastes*, IAEA, pp. 133–144.

Gy P. (1979) *Sampling of Particulate Materials: Theory and Practice*. Elsevier, Amsterdam, 431 pp.

Huertas F., Mayor J. C. and del Olmo C. (1992) *Textural and Fluid Phase Analysis of Rock Salt Subjected to the Combined Effects of Pressure, Heat and Gamma Radiation*. Nuclear Science and Technology EUR 14169 EN, 218 pp.

Hwang Y., Lee W. W. L., Chambré P. L. and Pigford T. H. (1989) *Mass Transport in Salt Repositories: Steady-state Transport Through Interbeds*. LBL-26704 Lawrence Berkeley Laboratory, 13 pp.

IAEA (1977) Site selection factors for repositories of solid high level and alpha-bearing wastes in geological formations. Tech. Rep. Series 177, 60 pp.

IAEA (1991) Guidelines for the operation and closure of deep geological repositories for the disposal of high level and alpha bearing wastes. *Tech. Doc.* 630, 32 pp.

Jain U. and Lidiard A. B. (1977) The growth of colloidal centres in irradiated alkali halides. *Phil. Mag.* **35**, 245–259.

Jenks G. H. (1979) *Effects of Temperature, Temperature Gradients, Stress and Irradiation on Migration of Brine Inclusions in a Salt Repository*. ORNL-5526, 62 pp.

Jenks G. H., Sonder E., Bopp C. D., Walton J. R. and Lindenbaum S. (1975) Reaction products and stored energy released from irradiated sodium chloride by dissolution and by heating. *J. Phys. Chem.* **79**, 871–875.

Jockwer N. (1981) Laboratory investigations of water content within rock salt and its behaviour in a temperature field of disposal high level waste. In *Scientific Basis for Nuclear Management* 3, pp. 35–40. Plenum.

Liptay G. (1971) *Atlas of Thermoanalytical Curves*, Vol. 1. Heyden & Son Ltd., 116 pp.

Ménager M. T., Petit J. C. and Brocard M. (1992) The migration of radionuclides in granite: a review based on natural analogues. *Appl. Geochem. Suppl.* **1**, 217–238.

Mönig J., García Celma A., Helmholdt R. B., Hinsch H., Huertas F. and Palut J. M. (1990) *The HAW Project: Test Disposal of High-level Waste in the Asse Salt Mine. International Test-plan for Irradiation Experiments*. Nuclear Science and Technology EUR 12946 EN, 76 pp.

Olander D. R. (1982) A model of brine migration and water transport in rock salt supporting a temperature gradient. *Nucl. Technol.* **58**, 256–270.

Ortí F. and Pueyo J. J. (1977) Asociación halita bandeada-anhidrita nodular del yacimiento de Remolinos, Zaragoza (sector central de la Cuenca del Ebro). Nota petrogenética. *Rev. Ins. Inv. Geol. Dip. Prov. Barcelona* **32**, 167–202.

Ortí F. and Pueyo J. J. (1983) Origen marino de la sal triásica del domo de Pinoso (Alicante, España). *Acta Geol. Hisp.* **18**, 139–145.

Pigford T. (1982) Migration of brine inclusions in salt. *Nucl. Technol.* **56**, 93–101.

Rios J. M. (1963) *Materiales Salinos del Suelo Español*. I.G.M.E. Mem **64**, 166 pp.

Roedder E. (1984) The fluids in salt. *Am. Mineral.* **69**, 413–439.

Roedder E. and Bassett R. L. (1981) Problems in determi-

nation of the water content of rock salt samples and its significance in nuclear waste storage siting. *Geology* **9**, 525–530.

Rothfuchs T. (1986) In situ investigations on the impact of heat production and gamma radiation with regard to high-level radioactive waste disposal in rock salt formations. *Nucl. Technol.* **58**, 256–270.

Schlich M. (1986) *Simulation der Bewegung von im natürlichen Steinsalz enthaltener Feuchte im Temperaturfeld.* GSF-Bericht 2/86, 246 pp.

Schlich M. and Jockwer N. (1985) Simulation of water transport in heated rock salt. *Mat. Res. Soc. Symp. Proc.* **50**, 577–585.

Schulze O. (1986) Der Einfluss radioaktiver Strahlung auf das mechanische Verhalten von Steinsalz. *Z. Geol. Ges.* **137**, 47–69.

Serrano A., Martinez del Olmo W. and Cámara P. (1989) Diapirismo del Trías Salino en el dominio Cántabro-Navarro. In *Libro Homenaje a Rafael Soler*, A.G.G.E.P., pp. 115–121.

Spiers C. J., Urai J. L., Lister G. S., Boland J. N. and Zwart H. J. (1986) *The Influence of Fluid–Rock Interaction in the Rheology of Salt Rock.* Nuclear Science and Technology EUR 10399 EN, 131 pp.

Urai J. L. (1983) Deformation of wet salt rocks. Ph.D. Thesis, Univ. Utrecht, 221 pp.

Vallet P. (1972) Thermogravimétrie. In *Monographies de Chimie Minerale*. Gauthier-Villars (Ed.), 385 pp.